JOURNAL OF GEOPHYSICAL RESEARCH, VOL. 112, A10206, doi:10.1029/2007JA012406, 2007

Quantitative estimates of magnetic field reconnection properties from electric and magnetic field measurements

F. S. Mozer[1] and A. Retinò[2]

Received 18 March 2007; revised 6 June 2007; accepted 13 July 2007; published 10 October 2007.

[1] Reconnection occurs in a reconnection magnetic field geometry when there are positive electric field components tangential to the magnetopause and a magnetic field component normal to it. Because these three components are the smallest of the six electric and magnetic fields, their magnitudes are difficult to determine because of errors in, or oscillations of, the assumed constant direction normal to the current sheet. A method is described for minimizing these errors by appropriate selection of the normal direction and by analyzing the correlations between the large normal electric field and the large tangential magnetic field. The correlation coefficients are equal to ratios of the small fields, which are combined with the less accurate measurements of the averages of the small fields to produce best estimates of the small fields. For more than 120 magnetopause crossings, about 40% had such correlations that signify static conditions during those crossings. This method is applied to 22 polar subsolar magnetopause crossings to show that most were located in the ion diffusion region, as defined by the change of the total magnetic field, and that 14 had a large and steady reconnection rate with a zero parallel electric field. In these events the reconnection rate decreased with increasing guide magnetic field.

Citation: Mozer, F. S., and A. Retinò (2007), Quantitative estimates of magnetic field reconnection properties from electric and magnetic field measurements, *J. Geophys. Res.*, *112*, A10206, doi:10.1029/2007JA012406.

1. Introduction

[2] Magnetic field reconnection is a multiscale process that may be investigated in three spatial domains, the electron scale, c/ω_{pe}, ($\sim$1 km at the subsolar magnetopause), the ion scale, c/ω_{pI}, ($\sim$50 km at the subsolar magnetopause) and the magnetohydrodynamic (MHD) scale, where c is the speed of light and ω_{pe} and ω_{pI} are the electron and ion plasma frequencies, respectively. The generalized Ohm's law of equation (1) may be invoked to determine in which of the three spatial regions an observation is made.

$$\mathbf{E} + \mathbf{U}_I x \mathbf{B} = c\mathbf{j}x\mathbf{B}/en - c\nabla \cdot \mathbf{P}_e/en + \left(m_e c^2/ne^2\right)\delta\mathbf{j}/\delta t + \eta\mathbf{j}, \quad (1)$$

where **E** and **B** are the electric and magnetic fields, $\mathbf{U}_I$ is the velocity of an element of ion fluid, **j** and n are the current and plasma densities, respectively, η is the resistivity associated with ion–electron interactions, and $\nabla \cdot \mathbf{P}_e$ is the divergence of the electron pressure tensor. If the terms on the right-hand side of equation (1) are all zero, one is in the MHD regime where both the ions and electrons are magnetized and their perpendicular flow is given by $\mathbf{E}x\mathbf{B}/B^2$. Therefore there is no perpendicular current so the current associated with the magnetic field reversal is parallel to the magnetic field, which results in the total magnetic field remaining unchanged during the crossing. This signature of a "constant" total magnetic field will be used to determine whether a measurement is or is not made in the MHD regime.

[3] The ion diffusion region is defined as the region in which the perpendicular ion motion is different from $\mathbf{E}x\mathbf{B}/B^2$ because the first term on the right side of equation (1), called the Hall MHD term, is significant. Thus in the ion diffusion region the total magnetic field changes across the current sheet and this signature will be used to determine if the spacecraft crossed the magnetopause through the ion diffusion region. By this definition, ion diffusion regions have been observed at huge distances from the reconnection X line at the separatricies in the solar wind [*Phan et al.*, 2006] so it should not be surprising to find them at many subsolar magnetopause crossings. In the electron diffusion region, some or all of the remaining terms on the right side of equation (1) are nonzero, so the electrons are unmagnetized and electric fields parallel to the magnetic field line occur. Experimental evidence on reconnection on the electron scale comes from such parallel electric field measurements [see *Mozer*, 2005, and references therein], while evidence of magnetic field reconnection on the MHD scale at the dayside magnetopause originally came from analyses of plasma observations and magnetic field data [*Paschmann et al.*, 1979; *Sonnerup et al.*, 1981], although statistical evidence from electric field measurements was also obtained [*Lindqvist and Mozer*, 1990]. The dividing lines

[1]Space Sciences Laboratory, Department of Physics, University of California, Berkeley, California, USA.
[2]Swedish Institute of Space Physics, Uppsala, Sweden.

0148-0227/07/2007JA012406$09.00

between the MHD regime and the ion diffusion region or between the ion diffusion region and the electron diffusion region are blurred by the likelihood that neither the perpendicular current nor the parallel electric field are ever exactly zero. This conceptual difficulty is ignored in the discussions that follow by discussing these regions in a qualitative sense.

[4] With the development of improved electric field detectors and analysis techniques, evidence of reconnection on the ion scale is now obtained from electric and magnetic field data at individual magnetopause crossings [*Mozer et al.*, 2002; *Vaivads et al.*, 2004; *Wygant et al.*, 2005]. However, this evidence is limited by uncertainties in the experimentally determined and assumed constant direction normal to the magnetopause. In this paper, examples of reconnection observed in electric and magnetic field data are presented and a new method of analysis is presented to minimize the uncertainty in the measurements arising from lack of exact knowledge of the appropriate coordinate system.

[5] Magnetic field reconnection requires the existence of electric field components of the proper sign tangential to the magnetopause and a magnetic field component normal to it [*Sonnerup*, 1979]. Nonzero tangential electric fields are required for the Poynting vector to have a nonzero integral over any closed surface (which means that electromagnetic energy is being converted) and for the $\mathbf{E}\mathrm{X}\mathbf{B}/B^2$ plasma flow to be inward from both sides. Also, in a static situation, the tangential electric field is a measure of the magnitude of the reconnection rate. The normal magnetic field is required for magnetic field lines on the two sides of the current sheet to connect through the current sheet. In a coordinate system having X normal to the current sheet, Y in the out-of-plane direction, and Z in the direction of the reconnecting magnetic fields (which is close to the GSE system for subsolar reconnection), the electric and magnetic fields E_X, B_Y, and B_Z are generally large and well measured while the required tangential electric fields, e_Y and e_Z, and normal magnetic field, b_X, are generally small. (In this paper, the normally large fields are capitalized and the normally small fields are represented in lowercase.) This makes the magnitudes of the small but most important fields susceptible to variations in the experimentally determined and assumed constant direction normal to the current sheet because such variations cause the large fields to have apparent components in the small field directions. A method will be introduced for obtaining information about the small fields from measurements of only the large fields. Because the large fields depend on the cosine of the small angular uncertainty of the normal direction, they are relatively uninfluenced by errors in the normal. Thus the small fields obtained by consideration of only the large fields are free of their major error source and are relatively well determined. Such determinations are required for more quantitative evidence of reconnection and for estimates of the reconnection rate.

2. Observations

[6] Processing of field data obtained on a satellite that crossed the magnetopause requires several steps. The electric fields must be translated into the magnetopause frame. The fields must also be rotated into a frame having one direction (the X direction) perpendicular to the current sheet, because it is only in this frame that one expects b_X, e_Y, and e_Z to be constant for steady state reconnection. The fields presented in this paper have all been translated and rotated using methods that are described in Appendix A. In practice, even after this translation and rotation, the magnitudes of the small fields vary considerably around their average values, so additional steps are required to extract best estimates of these average values and of the properties of reconnection that are deduced from them. Obtaining best estimates of the averages of the small fields is the central topic of the following discussions.

[7] Figures 1 and 2 present the fields at two subsolar magnetopause crossings in which reconnection will be shown to have occurred. Figures 1a and 2a give the plasma density as obtained from the spacecraft potential; Figures 1b and 2b give the magnetic field strength; Figures 1c–1e and 2c–2e present the three components of the magnetic field in the joint variance frame that is defined in Appendix A; Figures 1f–1h and 2f–2h give the three components of electric field in the same frame; and Figures 1i–1k and 2i–2k provide the three components of $\mathbf{E}\mathrm{X}\mathbf{B}/B^2$. The electric field was measured at a rate of 40 samples/s, the magnetic field was measured at 8 samples/s and the fields in both figures have been low-pass filtered at 0.5 Hz to eliminate the large amplitude electrostatic fluctuations that otherwise mask the features that will be discussed.

[8] Figures 1a and 1e show that the spacecraft passed from the magnetosphere, where the reconnecting component of the magnetic field, B_Z, was positive and the density was lower, into the magnetosheath where B_Z was negative and the density was higher. Figures 2a and 2e show that the spacecraft passed from the magnetosphere into the magnetosheath at ~0749 and back into the magnetosphere near 0750:20. In Figures 1b and 2b the magnetic field strength changed significantly, while in Figures 1c and 2c the reconnecting component, B_Z, changed, signifying that these crossings occurred in the ion diffusion region. It is noted that, in spite of the fact that the crossings were through the ion diffusion region where reconnection was occurring (as shown below), the out-of-plane magnetic field, B_Y, did not have a quadrupolar structure and the normal electric field, E_X, was not bipolar, as would be expected from symmetric simulations with no guide field [*Pritchett*, 2001]. In fact, of >120 subsolar magnetopauses that have been studied, there was an unambiguous bipolar E_X and quadrupolar B_Y in only one example [*Mozer et al.*, 2002]. About 20% of the crossings had a B_Y that peaked at the time when the reconnection magnetic field, B_Z, went through zero, which means that the magnetic field strength was roughly constant or that the transition was through the MHD region. The remainder of the crossings had an out-of-plane magnetic field that was unstructured.

[9] The data of Figure 1 were obtained from the three component measurements of the electric and magnetic fields at the radial distance of 9.28 R_E, the magnetic local time of 1320, and the magnetic latitude of 8.9°. They have been transformed from the spacecraft frame to the magnetopause frame by an X velocity of 20 km/s, which was determined from the condition that the average tangential component of the electric field was constant in the magnetopause frame. The time for crossing each of the two current sheets

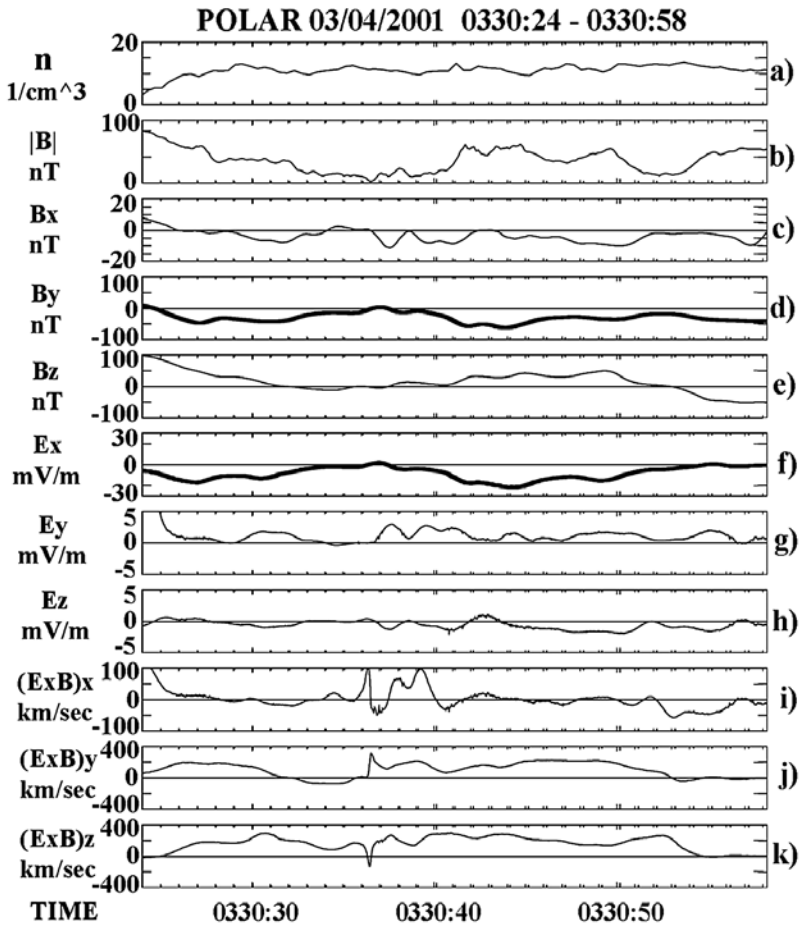

Figure 1. (a–k) A subsolar magnetopause crossing by the Polar satellite on 4 March 2001. Because the plasma density of Figure 1a increased with time, and the Z component of the magnetic field in Figure 1e decreased, this is a crossing from the magnetosphere into the magnetosheath. Because the tangential electric field of Figure 1g and the normal magnetic field of Figure 1c were nonzero, reconnection was occurring at this crossing. The remarkable correlation between the normal electric field of Figure 1f and the tangential magnetic field of Figure 1d provides important information on the reconnection rate.

evidenced by the major magnetic field changes in Figure 1e at 0330:24–0330:30 and 0330:50–0330:55 was about 5 s, which translates into their thicknesses being about 100 km or between 1 and 2 times c/ω_{pI}. This is further evidence that this crossing was through the ion diffusion region.

[10] The data of Figure 1 might be interpreted as a crossing at the beginning of the figure followed by a partial return toward the magnetosphere after the center of the figure and finally, passage into the magnetosheath near the end of the figure. If this was the case, the translation from the spacecraft frame to the magnetopause frame would not be at a constant velocity and the correct e_Y in the magnetopause frame near the center of Figure 1 would differ from that in the figure by less than 1 mV/m, which is small compared to the fluctuations of this component. It would not affect E_X, so the analyses below would be unmodified.

[11] The magnetopause crossing of Figure 2 occurred at the radial distance of 8.6 R_E, the magnetic local time of 1020, and the magnetic latitude of 10.3°. Because the spacecraft passed from the magnetosphere to the magnetosheath and back (see the magnetic field data in Figure 2e), the current sheet must have oscillated back and forth over the spacecraft and/or skimmed along it. In either case the average speed normal to the magnetopause must have been small. For this reason, it is assumed that the spacecraft and magnetopause frames were the same. This assumption is validated by the fact that e_Y of Figure 2g shows no change correlated with the variation of B_Z in Figure 2e, which it would have if the magnetopause speed changes affected the electric field translation.

[12] Below, the properties of the magnetopause crossings of Figures 1 and 2 are summarized:

[13] 1. In both cases, b_X in Figures 1c and 2c was negative, although the low-frequency oscillations of the data make the average magnitude of this component uncertain. Note the different amplitude scale for these figures as compared to that for B_Y and B_Z because b_X is nearly an order of magnitude smaller than B_Y or B_Z. The fluctuations in b_X are not instrumental because the uncertainty of the normal component of the magnetic field (that was mainly in the spin plane where the measurement accuracy is best) is ~0.1 nT (C/T. Russell, private communication, 2006). As discussed above, a nonzero average value of b_X is required at a reconnecting magnetopause.

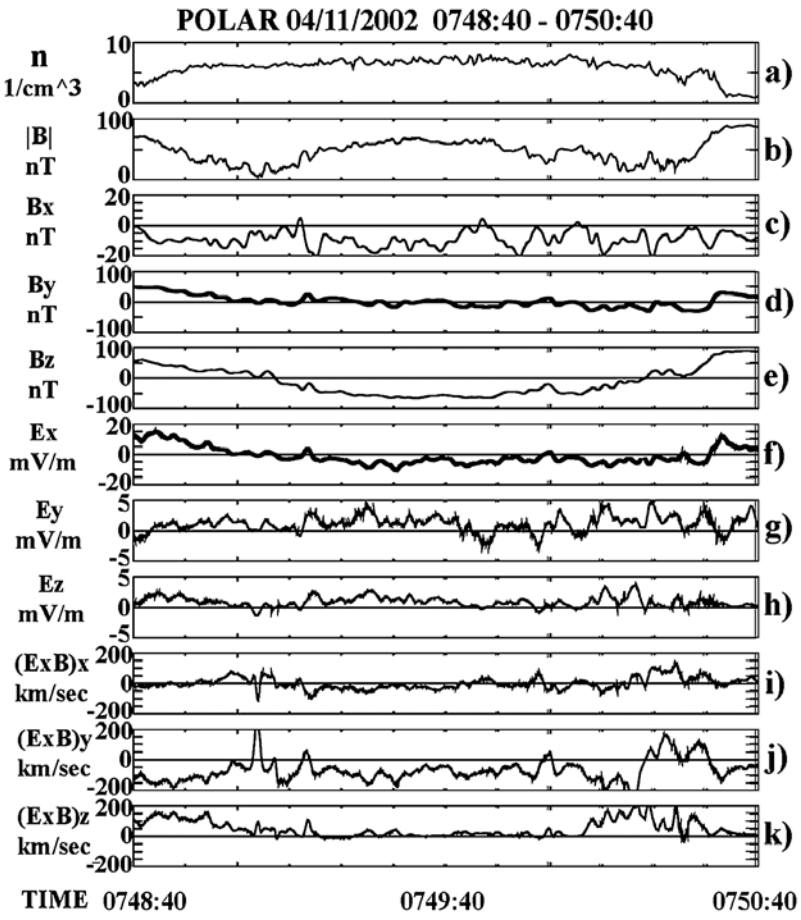

Figure 2. (a–k) A subsolar magnetopause crossing by the Polar satellite on 11 April 2002. Because the plasma density of Figure 2a increased and then decreased with time, and the Z component of the magnetic field in Figure 2e decreased and then increased, this is a crossing from the magnetosphere into the magnetosheath and back into the magnetosphere. Because the tangential electric field of Figure 2g and the normal magnetic field of Figure 2c were nonzero, reconnection was occurring at this crossing. The remarkable correlation between the normal electric field of Figure 2f and the tangential magnetic field of Figure 2e provides important information on the reconnection rate.

[14] 2. Because b_X is negative above and positive below the X line at the subsolar magnetopause, the negative average b_X in both figures means that the spacecraft should have passed through regions where the outflow in the Z direction was positive, as it was in Figures 1k and 2k.

[15] 3. The average value of e_Y in Figures 1g, 1h, 2g, and 2h are positive although the low-frequency oscillations make the magnitudes of these components uncertain. Note the different amplitude scales for these figures as compared to that for E_X, because E_X is almost an order of magnitude larger than e_Y or e_Z. The X and Z components of the electric field are accurate to better than 1 mV/m because these components were largely in the spacecraft spin plane. The Y component was measured by the on-axis sensor which has an uncertainty of about 1 mV/m for short time intervals such as that in Figure 1. However, over the longer time period of Figure 2, the uncertainty in the Y component is larger because the offset in the on-axis measurement depends on plasma parameters [*Mozer*, 2005] that varied more over the longer time interval. For this reason, the third component of the electric field in Figure 2 was determined by assuming that the parallel electric field was zero. (The average difference between the two values of e_Y was less than 2 mV/m.) The assumption that the parallel electric field is zero provides the more accurate approach because, as will be shown, the parallel electric field was measured to be consistent with zero over the magnetopause crossing by a method that is independent of this assumption. (This independence follows because the only electric field component involved in the method is E_X and this component is not affected by the assumption that the parallel field is zero because the spacecraft spin axis was in the Y direction.) For both magnetopause crossings, the average tangential electric field was greater than the experimental uncertainties and the fluctuations of the tangential electric field were real. A positive value of the tangential electric field is necessary for reconnection to occur. In spite of the oscillations of the small fields, $(\mathbf{E}\mathrm{X}\mathbf{B}/B^2)_X$ in Figures 1i and 2i is inward from both sides, as is necessary for reconnection. It is noted that $(\mathbf{E}\mathrm{X}\mathbf{B}/B^2)_X$ varies across the magnetopause, as expected, and this variation is unrelated to reconnection properties

Table 1. Parameters of Two Reconnection Events

Event	R^2	a	b	c
4 Mar 2001	0.990	−0.33	0.16	−0.07
4 Mar 2001	0.977	−0.24	0.13	≡0
11 Apr 2002	0.903	−0.19	−0.07	0.03
11 Apr 2002	0.836	−0.16	−0.08	≡0

which are better studied by considering the average values of the small fields.

[16] 4. The Alfvén speed based on magnetosheath parameters for Figure 1 was 330 km/s while that based on magnetospheric parameters was 1120 km/s, and the observed $(\mathbf{E}\mathrm{X}\mathbf{B}/B^2)_Z$ in Figure 1k had a magnitude of 350 km/s. For Figure 2 the corresponding Alfvén speeds were 520 and 1110 km/s while the observed $(\mathbf{E}\mathrm{X}\mathbf{B}/B^2)_Z$ in Figure 2k had a magnitude of 200 km/s. The observed speeds are consistent with alfvenic outflow at a reconnecting magnetopause although they give only the perpendicular component of the outflow.

[17] 5. In Figure 2k, the outflow coincided in time with the out-of-plane current associated with the changing magnetic field component of Figure 2e. This frequently observed correlation follows from the major part of the electromagnetic energy conversion occurring at such locations because this is where $(\mathbf{j}\cdot\mathbf{E})_Y$ is largest.

[18] 6. In both figures, there is a strong correlation between E_X of Figures 1f and 2f and B_Y of Figures 1d and 2d. Such observed correlations have been noted earlier [*Mozer et al.*, 2002; *Wygant et al.*, 2005]. In fact, to the eye, about 40% of >120 crossings exhibited correlations of E_X with B_Y or B_Z, which, as discussed below, shows that the fields were static during those crossings.

3. Analyses of Correlations

[19] The method for obtaining the small fields, e_Y, e_Z and b_X from the correlations between E_X and B_Y or B_Z is next discussed. Consider the condition imposed on the fields by the definition of the parallel electric field, which is:

$$E_X b_X + e_Y B_Y + e_Z B_Z = e_{ll} B_{total}, \tag{2}$$

where e_{ll} is the parallel electric field. If reconnection is not occurring and b_X, e_Y, e_Z, and e_{ll} are zero, equation (2) is satisfied for arbitrary values of E_X, B_Y, and B_Z, so there is no necessary correlation between these large fields. However, if reconnection is occurring and the small fields are therefore nonzero,

$$E_X = -(e_Y/b_X)B_Y - (e_Z/b_x)B_Z + (e_{ll}/b_x)B_{total}. \tag{3}$$

In this case, E_X is correlated with B_Y and B_Z by factors that are given by the small fields including the parallel electric field. If it is further assumed that the ratios of the small fields are constant, as is required in a static, planar magnetopause frame and as will be shown by the analyses that follow, equation (3) may be written

$$E_X = -aB_Y - bB_Z + cB_{total}, \tag{4}$$

where the constants a, b, and c are given as $a = (e_Y/b_X)$, $b = (e_Z/b_X)$, and $c = (e_{ll}/b_x)$.

[20] As an aside, if c is set equal to zero, equation (4) is identical to the X component of

$$\mathbf{E} + \mathbf{v}\mathrm{x}\mathbf{B} = 0, \tag{5}$$

where $\mathbf{v}$ is the deHoffmann-Teller velocity that transforms the electric field into a frame where it is zero [*Khrabrov and Sonnerup*, 1998]. The deHoffmann-Teller formulation has been used for the purpose of testing whether some magnetopause crossings were rotational discontinuities [*Aggson et al.*, 1983]. Neither this nor any subsequent work has utilized the fact that the deHoffmann-Teller velocity is related to the small field components, and this relationship will be exploited here in the form of equation (4) to produce more accurate estimates of the normal magnetic field, the tangential electric field, the parallel electric field and the reconnection rate.

[21] Using least squares analyses, equation (4) has been tested on 22 subsolar magnetopause crossings. The results for the data of Figures 1 and 2 are given in Table 1.

[22] The first row of data in this table for each date was obtained by allowing c $(=e_{ll}/b_x)$ to be determined by the least squares method while the second row assumes that c (and e_{ll}) were zero. Because c is found to be nearly an order of magnitude smaller than a, which means that the parallel field was nearly an order of magnitude smaller than the tangential electric field and two orders of magnitude smaller than the normal electric field and because its value is not statistically different from zero, it is concluded that the average e_{ll} was consistent with zero for these crossings. The statistical uncertainties in the values of a and b are very small so their uncertainties are better estimated as about 10% from the differences that were found by changing the interval over which the least squares fits were calculated.

[23] The correlation coefficient, R^2, is the fraction of the total squared error that is explained by the model. This means, for example, that 97.7% of the E_X variance in the second row of Table 1 is accounted for by equation (4). Plots of the left and right sides of equation (4) are given in Figures 3a and 4a for the two events and for the case that $e_{ll} = 0$. That the right side of equation (4), with its constant coefficients, describes the measured E_X values to the observed accuracies, is a strong statement that the geometry and small field ratios were constant during both crossings. Because b_X was shown to be negative from both its average value and from the fact that the Z component of $\mathbf{E}\mathrm{x}\mathbf{B}/B^2$ was positive, and because the quantity a was negative in Table 1, it follows that the tangential component of the electric field was positive in both cases, so reconnection at a constant rate was occurring at these crossings.

[24] The ratio of the measured e_Y/b_X is compared with the least squares coefficient, a, and the measured e_Z/b_X is compared with the least squares coefficient, b, in Figures 3b, 3c, 4b, and 4c, in which the field ratios were plotted only when e_Y/b_X and e_Z/b_X did not diverge owing to large E fields or small b_X. In all cases, there is an average agreement between the measured ratios and those determined from the least squares fits. The differences between the model and measured quantities in Figures 3b, 3c, 4b, and 4c exceed experimental uncertainties, so there must be another expla-

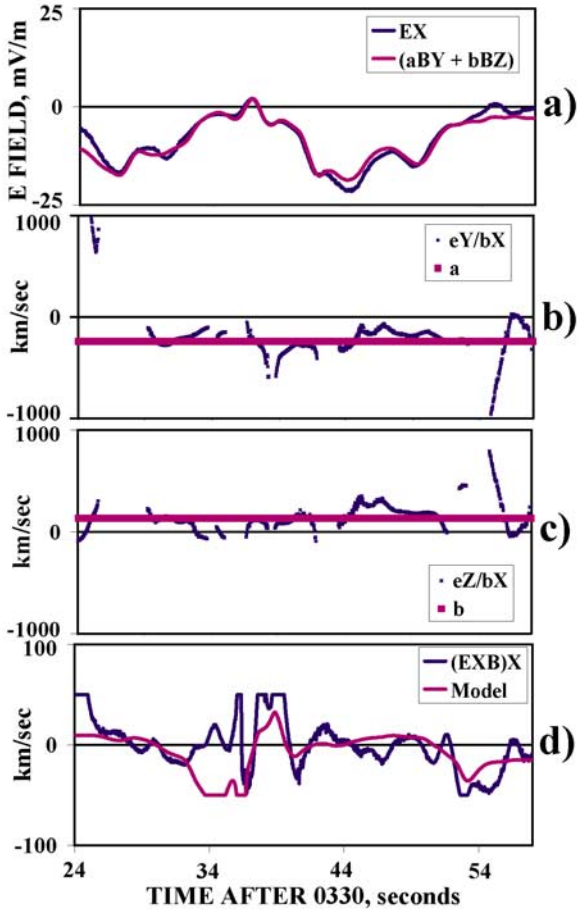

Figure 3. (a–d) Comparison of least squares fit parameters and field measurements on 4 March 2001.

nation of the discrepancy. The most plausible explanation is that the analysis of the satellite data assumes that the normal to the current sheet is fixed in direction while, in reality, it may oscillate through angles of several degrees owing to surface undulations of the magnetopause. Such undulations cause a portion of the large fields to appear as if they were small fields in the analysis that assumes a fixed normal direction, even though the actual small field ratios are constant, as deduced from the quality of the least squares fits described below. This interpretation means that the reconnection rates and geometry were constant for both crossings even though the boundary normal oscillated and, in the latter case, the magnetopause moved back and forth over the spacecraft.

4. Best Values

[25] For each magnetopause crossing, there are five measurements $\langle e_Y \rangle$, $\langle e_Z \rangle$, $\langle b_X \rangle$, a, and b, of three quantities, $\mathbf{e_Y}$, $\mathbf{e_Z}$, and $\mathbf{b_X}$, where $\langle e_Y \rangle$, $\langle e_Z \rangle$, and $\langle b_X \rangle$ are the average values of the measured small fields and the bold lowercase fields are the best estimates of the small fields, as deduced from the following analysis. The coefficients a and b are the most accurate because they are insensitive to the direction or fluctuations of the normal to the current sheet. However, they provide information on ratios of the small fields and not on the small fields themselves. An ad hoc procedure must be defined to produce the "best" estimate of the three fields from the five measurements. These three fields will be obtained from the five measurements by minimizing the function

$$f = (\Delta e_Y/\mathbf{e_Y})^2 + (\Delta e_Z/\mathbf{e_Z})^2 + (\Delta b_X/\mathbf{b_X})^2, \tag{6}$$

where

$$\Delta e_Y \equiv \mathbf{e_Y} - \langle e_Y \rangle \tag{7a}$$

$$\Delta e_Z \equiv \mathbf{e_Z} - \langle e_Z \rangle \tag{7b}$$

$$\Delta b_X \equiv \mathbf{b_X} - \langle b_X \rangle. \tag{7c}$$

Assuming that a and b are error-free and substituting $a = \mathbf{e_Y}/\mathbf{b_X}$ and $b = \mathbf{e_Z}/\mathbf{b_X}$ gives

$$\Delta e_Z = b/a(\langle e_Y \rangle + \Delta e_Y) - \langle e_Z \rangle \tag{7d}$$

$$\Delta b_X = (\langle e_Y \rangle + \Delta e_Y)/a - \langle b_X \rangle, \tag{7e}$$

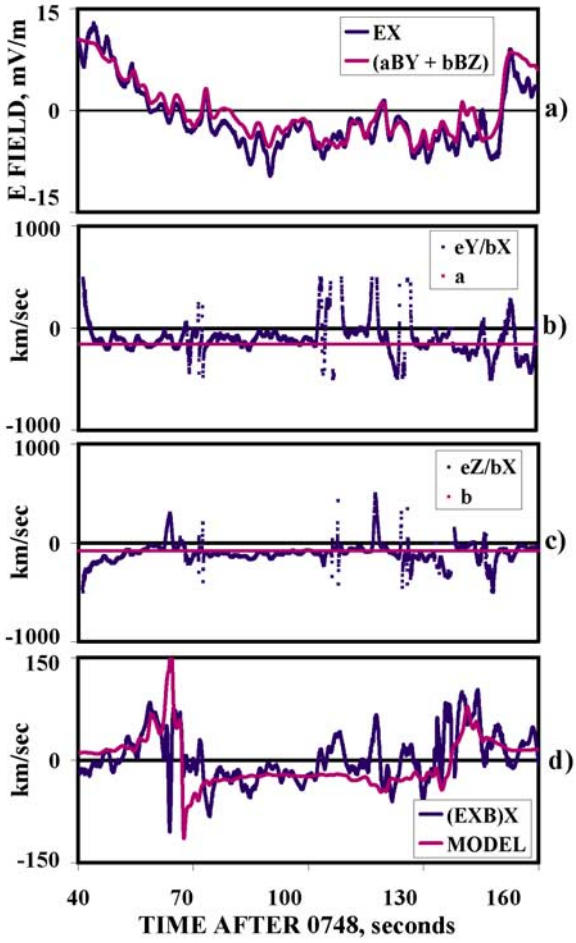

Figure 4. (a–d) Comparison of least squares fit parameters and field measurements on 11 April 2002.

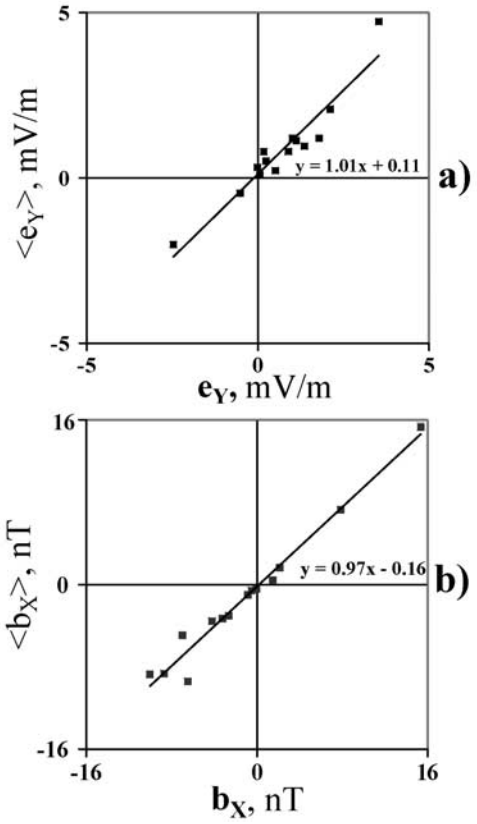

Figure 5. (a and b) Comparison of $\langle e_Y \rangle$ with $\mathbf{e_Y}$ and $\langle b_X \rangle$ with $\mathbf{b_X}$. The solid lines and equations come from linear least squares fits.

and the function, $f(\Delta e_Y)$, to be minimized by setting $df(\Delta e_Y)/d\Delta e_Y = 0$ becomes

$$f(\Delta e_Y) = [\Delta e_Y/a]^2 + [(\langle e_Y \rangle + \Delta e_Y)/b - \langle e_Z \rangle/b]^2 + [(\langle e_Y \rangle + \Delta e_Y)/a - \langle b_X \rangle]^2, \quad (8)$$

to give Δe_Y, from which the best estimates of $\mathbf{e_Y}$, $\mathbf{e_Z}$, and $\mathbf{b_X}$ are obtained via equations (7a)–(7e).

[26] Comparisons of $\langle e_Y \rangle$ with $\mathbf{e_Y}$ and $\langle b_X \rangle$ with $\mathbf{b_X}$ are given in Figures 5a and 5b for the 14 magnetopause crossings having absolute values of coefficients a and b greater than 0.075. The remarkable fact that the averages of time varying quantities, such as those in Figures 1c, 1g, 2c, and 2g, agree with values deduced from the correlations of E_X with B_Y and B_Z to within standard deviations of 1.1 nT and 0.43 mV/m, attests both to the validity of the analysis methods and the accuracy of the original measurements.

[27] Two calculations of $(\mathbf{EXB}/B^2)_X = (e_Y B_Z - e_Z B_Y)/B^2$ are given in Figures 3d and 4d, where, in one case the measured small fields were used in the evaluation, and, in the other case, $\mathbf{e_Y}$ and $\mathbf{e_Z}$ were used. Both calculations for both crossings show that the plasma and electromagnetic energy flowed toward the center of the current sheet from each side, so reconnection was occurring. In Figure 3 this is evidenced by the opposite signs of the x component flows at the two ends of Figure 3d while in Figure 4 the flow in the center is opposite in sign to that at the ends of the plot because the spacecraft passed from the magnetosphere to the magnetosheath and back into the magnetosphere.

[28] Of the 22 events in this study, 14 were in the ion diffusion region because reconnection was occurring and the average $\Delta B/B$ was 0.3, where ΔB is the standard deviation from the average measured total magnetic field, B. Five of the events were in the MHD regime because the average $\Delta B/B$ was 0.09 and there was no reconnection. The remaining three events occurred in the ion diffusion region (the average $\Delta B/B$ was 0.33) but reconnection was not occurring (because $\mathbf{e_Y}$ was negative or zero). Average values of quantities determined from the 11 of 14 reconnection events having absolute values of the least squares coefficients a and b greater than 0.075 are given in Tables 2a and 2b.

[29] The average correlation coefficient in Table 2a was remarkably large and the excellent agreement between the average measured fields and those obtained from the correlations is testimony to the quality of the procedures. It is also noted that the average $\mathbf{e_Y}$ is three times the average $\mathbf{e_Z}$ and that the average $(\mathbf{EXB}/B^2)_Z$ outflow speed during the 11 reconnection events was the order of the Alfven speed.

5. Reconnection Rate

[30] To discuss the reconnection rate, consider the case of no guide magnetic field. The number of field lines entering the magnetopause along a unit length of the magnetopause is equal to the product of the field line density, B_Z, times the inflow speed, e_Y/B_Z. Thus the number of entering field lines per unit length per unit time is equal to the tangential electric field. In the more complex case of a nonzero guide magnetic field, the averages of Table 2b show that the product of the average B_Z and $(\mathbf{EXB}/B^2)_X$ was 1.04 mV/m at the magnetosheath and 0.99 mV/m at the magnetosphere. The fact that the magnitude of B_Z was larger in the magnetosphere than in the magnetosheath in Table 2b is compensated for by the fact that the average $(\mathbf{EXB}/B^2)_X$ was larger in the magnetosheath, such that the number of field lines entering from the two sides was equal to 4%. This average inflow rate was also equal to the average tangential electric field to within about 10%, which again attests to the validity of the analyses. Earlier estimates of the tangential electric field [*Sonnerup et al.*, 1990; *Lindqvist and Mozer*, 1990; *Phan et al.*, 2001; *Mozer et al.*, 2002; *Vaivads et al.*, 2004] compare well with the 1.16 mV/m average value found in this study.

[31] A scatterplot of $\mathbf{e_Y}$ versus B_G/B_Z for the 11 reconnection events having least squares coefficients greater in magnitude than 0.075 is given in Figure 6. B_G/B_Z is equivalent to the clock angle because B_G/B_Z is 0 for an 180° clock angle and it increases as the clock angle decreases. The data are consistent with a decrease of the reconnection rate with increasing guide field and with the reconnection rate becoming small as B_G/B_Z approaches 2.

[32] The reconnection rate is often defined as a dimensionless quantity by considering it to be the ratio of the inflow speed to the asymptotic Alfven speed. In the case of

Table 2a. Average Values of Parameters Measured in Eleven Reconnection Events

Parameter	Value
R^2 of the correlation	0.901
$\langle b_X \rangle$, nT	−3.21
$\mathbf{b_X}$, nT	−3.13
$\langle e_Y \rangle$, mV/m	1.25
$\mathbf{e_Y}$, mV/m	1.16
$\langle e_Z \rangle$, mV/m	0.33
$\mathbf{e_Z}$, mV/m	0.33

a zero guide magnetic field, the Alfven speed is $B_Z/(nm)^{1/2}$, where m is the ion mass, so the ratio of the inflow speed to the Alfven speed is

$$\text{reconnection rate} = \mathbf{e_Y}(nm)^{1/2}/B_Z^2. \quad (9)$$

Because, in the MHD regime, $e_Y = v_n B_Z$, where v_n is the Alfven speed based on the normal magnetic field, b_X, equation (9) is also

$$\text{reconnection rate} = \mathbf{b_X}/B_Z. \quad (10)$$

Thus for real data there are two ways of estimating the reconnection rate at each of the two asymptotic regions, so four estimates of the reconnection rate may be obtained from the data.

[33] For the case of a nonzero guide magnetic field, B_G, B_Y is nonzero in the asymptotic regions and the expressions for plasma and field line flows and the Alfven speed become more complicated. Thus the definition of the reconnection rate must be generalized. Fortunately, this issue is avoided in the present data set and equations (9) and (10) are used as the definition of the reconnection rate because the results obtained from the equivalent equations using the full magnetic field differ from the results of equations (9) and (10) by less than 15% on the average, which is small compared to the differences of the four estimates obtained from equations (9) and (10). Figure 7a is a plot of the reconnection rate computed four ways from these equations for each event. It includes the eight events having a zero reconnection rate in order to emphasize that some events do not display reconnection. Figure 7b is a histogram of the 44 reconnection rates estimated from the 11 magnetopause crossings having reconnection with least squares coefficients a and b greater than 0.075. The average of these data is a dimensionless reconnection rate of 0.072. If all 22 events are considered, the average reconnection rate is 0.046. An accurate value of the dimensionless reconnection rate is not as important as noting that it is several percent of the input Alfven speed, because such a reconnection rate eliminates the possibility that these events are

Table 2b. Average Values of Magnetosheath and Magnetosphere Parameters Measured in Eleven Reconnection Events

	Magnetosheath	Magnetosphere
$(\mathbf{EXB}/B^2)_X$, km/s	−23.8	14.6
$(\mathbf{EXB}/B^2)_Z/V_{Alfven}$	0.79	0.24
B_Z, nT	−43.5	68.0
$\lvert B_G/B_Z \rvert$	0.72	0.32

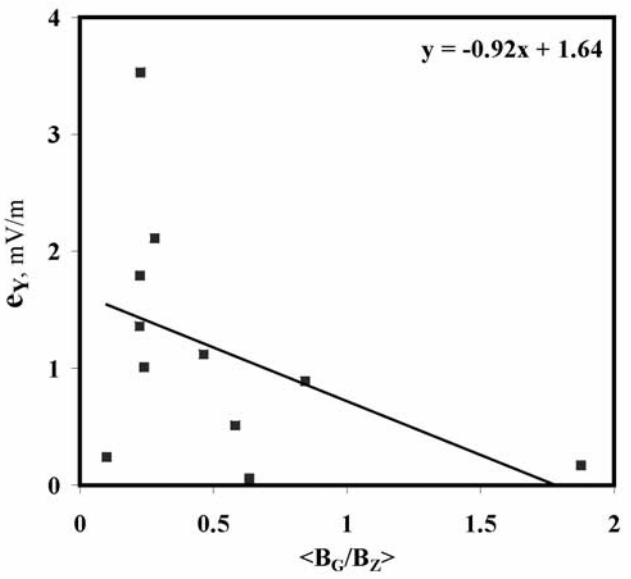

Figure 6. Comparison of $\mathbf{e_Y}$ and B_G/B_Z. The solid line and equation come from a linear least squares fit.

consistent with the Sweet-Parker model. It is not possible to search for reconnection rates consistent with this model because the errors in the measurements of the field are larger than the fields that would be expected in this model.

6. Other Examples

[34] Figures 8 and 9 present two examples from the data set of 22 events in the same format as Figures 1 and 2. The

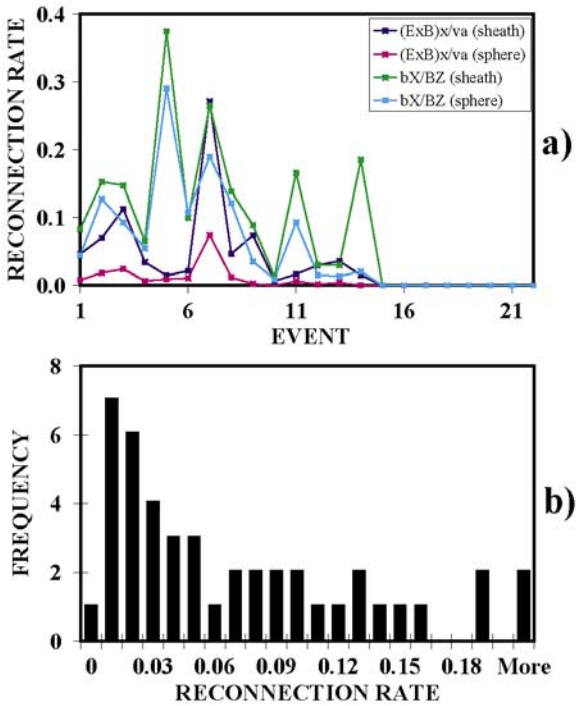

Figure 7. (a) Four values of the reconnection rate for each of the 22 events and (b) histogram of the reconnection rates for the 11 events that had reconnection with least squares coefficients a and b having magnitudes greater than 0.075.

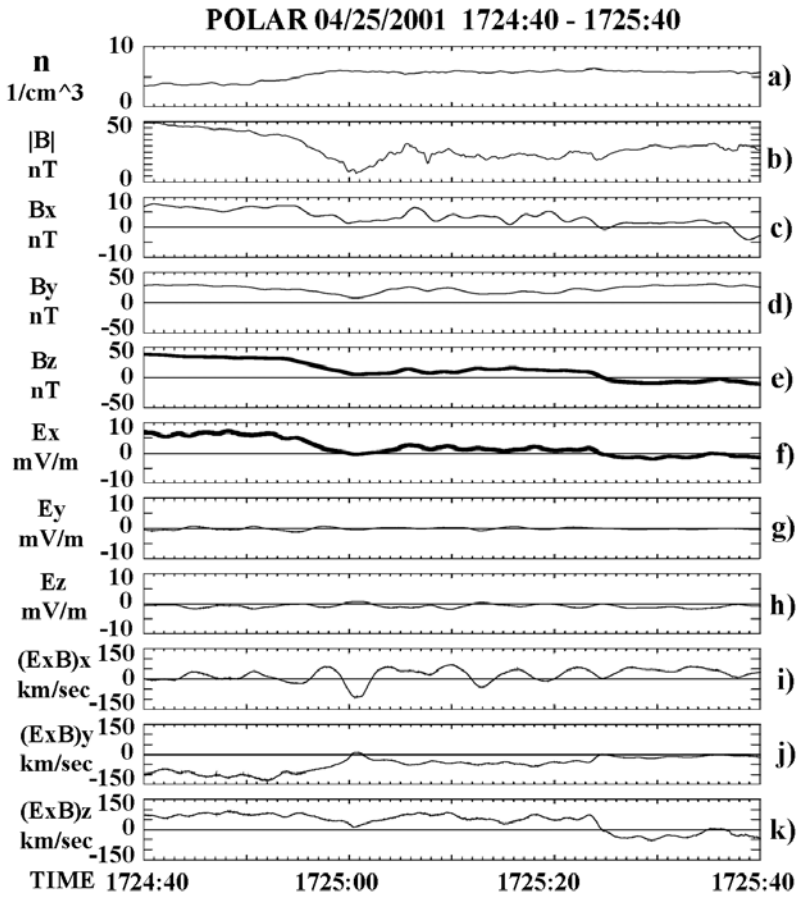

Figure 8. (a–k) Event of 25 April 2001 in the ion diffusion region with no reconnection. The large change of the total magnetic field in Figure 8b signifies that the observations were made in the ion diffusion region. The absence of reconnection is indicated by the small values of the tangential electric fields of Figures 8g and 8h, the absence of plasma and magnetic field inflow in Figure 8i, and the small outflow velocity in Figure 8k.

data of Figure 8 were obtained on 25 April 2001 at a geocentric distance of 9.47 R_E, a magnetic local time of 1010, and a magnetic latitude of 32.7°. The spacecraft was clearly in the ion diffusion region because the major change of the magnetic field strength in Figure 8b shows the presence of a perpendicular current and of the c**j**x**B**/en term in the Generalized Ohm's law. The spacecraft passed from the magnetosphere, where the density was low in Figure 8a and the reconnection magnetic field of Figure 8e was positive, to the magnetosheath, where the density was greater and the reconnecting field was negative. The fields e_Y, e_Z, and b_X were constant for this event as is suggested by the eyeball correlation between E_X of Figure 8f and B_Z of Figure 8e, and as is shown by the value of R^2, which was 0.956. However, reconnection did not occur at this crossing and location, as is known from the following:

[35] 1. $(\mathbf{E}\mathrm{X}\mathbf{B}/B^2)_X$ of Figure 8i was generally positive, so plasma and magnetic field lines generally flowed through the magnetopause in the positive X direction.

[36] 2. $(\mathbf{E}\mathrm{X}\mathbf{B}/B^2)_Z$ of Figure 8k was small and generally positive while the average value of b_X in Figure 8c was also positive. Thus the small outflow was in a direction not consistent with reconnection, as judged from the sign of b_X.

[37] 3. E_X of Figure 8f was everywhere less than 6 mV/m, and $\mathbf{e_Y}$ was −0.04 mV/m. These fields are among the smallest observed in the 22 events and are insufficient to support a significant reconnection rate.

[38] Thus the conclusion from Figure 8 is that, although the spacecraft was in the ion diffusion region and the small fields were constant, reconnection did not occur locally. This is a specific example of the general facts that it is possible to have perpendicular currents in a plasma without having reconnection and that a high correlation between the electric and magnetic fields only shows that the small fields were constant and not that reconnection occurred.

[39] The data in Figure 9 were obtained on 20 April 2002 at a geocentric distance of 7.34 R_E, a magnetic local time of 1020, and a magnetic latitude of 21.5°. The spacecraft passed from the magnetosheath, where B_Z was negative in Figure 9e and for the preceding 10 min, into the magnetosphere, where B_Z was positive at the end of Figure 9e and for the following 10 min. The plasma density of Figure 9a decreased about 50% during the interval shown and fell to less than 1 cm^{-3} a few minutes later, after passage through the boundary layer. Because the magnetic field strength in Figure 9b was essentially constant ($\Delta B/B = 0.03$), the current was largely field-aligned and the c**j**x**B**/en term of

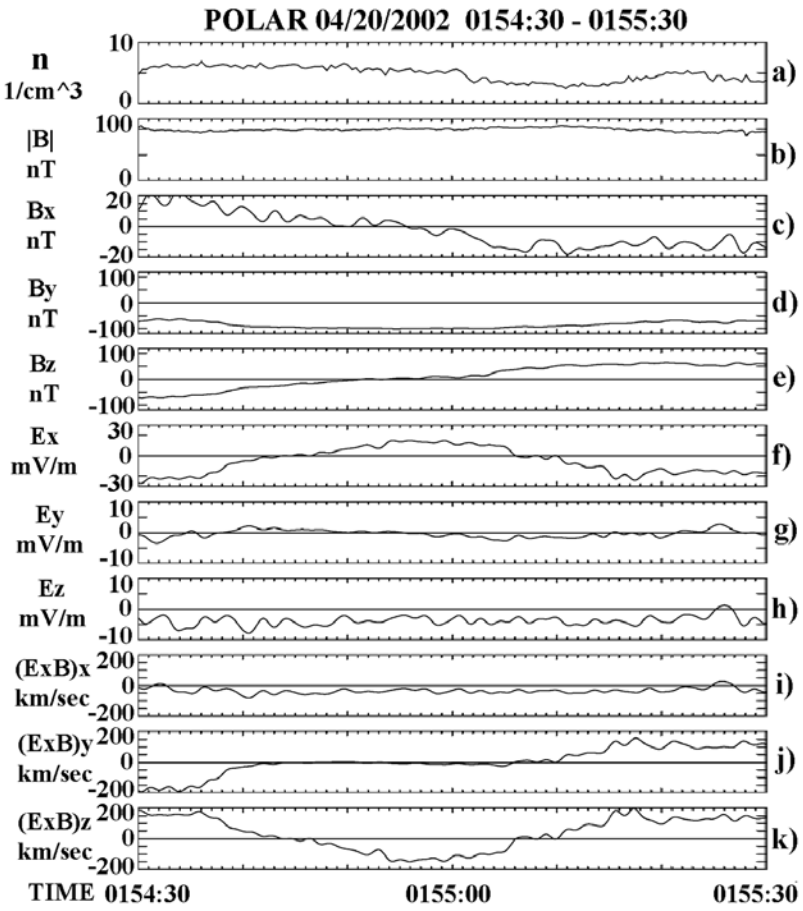

Figure 9. (a–k) Event of 20 April 2002. The crossing was made from the magnetosheath to the magnetosphere according to the change of B_Z in Figure 9e. The unimportant variation of the total magnetic field of Figure 9b indicates that the crossing was made in the magnetohydrodynamic regime. As shown in Figure 9i, there is no net inflow of plasma or magnetic field lines, so reconnection was not occurring at the location of the crossing.

equation (1) was small, so the spacecraft traversed the local magnetopause, including the separatricies, in the MHD regime. This conclusion is supported by the fact that $(\mathbf{EXB}/B^2)_X$ in Figure 9i was negative throughout the crossing such that the plasma and magnetic field lines flowed through the magnetopause in the negative direction and did not reconnect. In addition, e_Y was $\sim$0 and e_Z was negative, which is further proof that reconnection was not occurring at the satellite location. However, this event suggests that reconnection occurred elsewhere along this magnetopause.

7. Conclusions

[40] We have presented a method for investigating magnetic reconnection using electric and magnetic field measurements. We define reconnection as ongoing at a planar, stationary current sheet when positive tangential electric field components and a normal magnetic field component are present. The analysis method uses the observed correlations between the normal electric field, E_X, and the tangential magnetic fields, B_Y and B_Z, to obtain improved estimates of $\mathbf{e_Y}$, $\mathbf{e_Z}$, and $\mathbf{b_X}$, and to thereby provide quantitative evidence of reconnection. We find that steady state reconnection occurs in more than 60% of the 22 events that were studied. The method also shows that the parallel electric field is on average zero at ion scales. It is also found that the reconnection electric field decreases with increasing guide magnetic field and that the average reconnection rate is about 6%. The observation of apparent correlations in some 40% of >120 magnetopause crossings that were examined cursorily suggests that steady state reconnection may occur at a significant number of subsolar magnetopauses.

Appendix A: Joint Variance Analysis

[41] Methods for determining the coordinate frame of the current sheet from magnetic and electric field data include:

[42] 1. Minimum variance analysis of the magnetic field.

[43] 2. Maximum variance analysis of the electric field after transforming to the magnetopause frame.

[44] 3. Faraday residue method that uses both the electric and magnetic field data.

[45] The minimum variance method best locates the direction of the maximum varying magnetic field component, which is B_Z. The maximum variance method best locates the direction of the maximum varying electric field component, which is E_X [*Paschmann et al.*, 1990]. The Faraday residue method finds compromise directions for the various components. For the present purposes, the most

Table 3. Polar Data on 4 March 2001 From 0330:24 to 0330:58

Quantity	Minimum Variance	Maximum Variance	Joint Variance
$\langle b_X \rangle$, nT	−2.16	−3.53	−3.53
$\langle e_Y \rangle$, mV/m	0.67	1.24	1.21
$\langle e_Z \rangle$, mV/m	−0.80	−0.43	−0.55
$\langle e_Y \rangle / \langle b_X \rangle$	−0.31	−0.36	−0.34
$\langle e_Z \rangle / \langle b_X \rangle$	0.37	0.12	0.15
a	−0.24	−0.25	−0.24
b	0.13	0.11	0.13

important direction is the normal to the current sheet because this best separates E_X from e_Y and e_Z and best separates b_X from B_Y and B_Z. To emphasize this most important direction, a joint variance analysis method is introduced in which the normal direction is given by the maximum variance of the electric field. The coordinate system is then rotated about this axis until the Z direction is closest to the Z axis found from the minimum variance of the magnetic field. The rotation matrices from GSE to the magnetopause frame for the data of Figure 1 are as follows.

[46] For the minimum variance analysis:

$$\begin{matrix} 0.92929 & 0.36934 & 0.00325 \\ -0.34916 & 0.88132 & -0.31838 \\ -0.12045 & 0.29473 & 0.94796 \end{matrix}$$

[47] For the maximum variance analysis:

$$\begin{matrix} 0.90114 & 0.43337 & 0.1184 \\ -0.39206 & 0.82627 & -0.40443 \\ -0.18505 & 0.35981 & 0.91449 \end{matrix}$$

[48] For the joint variance analysis:

$$\begin{matrix} 0.90114 & 0.43337 & 0.1184 \\ -0.40752 & 0.85607 & -0.31794 \\ -0.14792 & 0.28168 & 0.94804 \end{matrix}$$

[49] The angle between the maximum variance X axis and the minimum variance Z axis is 88.3°. The angle between the X axes determined from the minimum and maximum variance analyses is 4.0°. The large effect of this difference is illustrated in Table 3.

[50] In Table 3, the values of the least squares coefficients a and b do not depend on the analysis method. This is because these coefficients are based on the three big field components which do not change appreciably for small angular changes of the coordinate system. It is also noted that $\langle e_Z \rangle / \langle b_X \rangle$ differs from b by a factor of three for the minimum variance analysis but it is approximately equal to b for the joint variance analysis. This is evidence that the best estimate of parameters comes from the joint variance analysis. Lastly, $\langle e_Y \rangle$ differs by a factor of two between the minimum and joint variance analyses owing to the above mentioned 4° difference. Thus the apparent error in the magnitude of the tangential electric field obtained from the minimum variance analysis is a factor of two in this and many other cases.

[51] It is noted that the rotation to the maximum variance frame is from the frame tied to the magnetopause and not to the spacecraft. Transformation to the magnetopause frame is obtained iteratively by first performing a maximum variance analysis on data in the spacecraft frame, then transforming to the magnetopause frame by a velocity in the X direction, and then doing a second maximum variance analysis. This procedure assures that the X-axis velocity transformation is in the approximately correct direction for the final coordinate rotation. For the case of Figure 1, the difference between the X directions in the two frames is 2.3° which means that a negligible 0.8 km/s of the 20 km/s translation velocity was not in the desired X direction.

[52] **Acknowledgments.** The authors thank C. T. Russell for his unselfish sharing of the magnetic field data from the Polar satellite and T. Phan for helpful discussions. This work was performed under NASA grant NNG05GC72G-01/08. A. Retinò was supported by the Swedish National Space Board.

[53] Amitava Bhattacharjee thanks both referees for their assistance in evaluating this paper.

References

Aggson, T. L., P. J. Gambardella, and N. C. Maynard (1983), Electric field measurements at the magnetopause: Observation of large convective velocities at rotational magnetopause discontinuities, *J. Geophys. Res.*, *88*, 10,000.

Khrabrov, A. V., and B. U. O. Sonnerup (1998), deHoffmann-Teller analysis, in *Analysis Methods for Multi-Spacecraft Data*, edited by G. Paschmann and P. W. Daly, p. 221, Eur. Space Ag., Paris.

Lindqvist, P.-A., and F. S. Mozer (1990), The average tangential electric field at the noon magnetopause, *J. Geophys. Res.*, *95*, 17,137.

Mozer, F. S. (2005), Criteria for and statistics of electron diffusion regions associated with subsolar magnetic field reconnection, *J. Geophys. Res.*, *110*, A12222, doi:10.1029/2005JA011258.

Mozer, F. S., S. D. Bale, and T. D. Phan (2002), Evidence of diffusion regions at a subsolar magnetopause crossing, *Phys. Rev. Lett.*, *89*(1), 015002, doi:10.1103/PhysRevLett.89.015002.

Øieroset, M., T. D. Phan, M. Fujimoto, R. P. Lin, and R. P. Lepping (2007), In situ detection of collisionless reconnection in the Earth's magnetotail, *Nature*, *412*, 414, doi:10.1038/35086520.

Paschmann, G., I. Papamastorakis, N. Sckopke, G. Haerendel, B. U. O. Sonnerup, S. J. Bame, J. R. Asbridge, J. T. Gosling, C. T. Russell, and R. C. Elphic (1979), Plasma acceleration at the Earth's magnetopause: Evidence for reconnection, *Nature*, *282*, 243.

Paschmann, G., B. U. O. Sonnerup, I. Papamastorakis, W. Baumjohann, N. Sckopke, and H. Lühr (1990), The magnetopause and boundary layer for small magnetic shear: Convection electric fields and reconnection, *Geophys. Res. Lett.*, *17*, 1829.

Phan, T. D., B. U. O. Sonnerup, and R. P. Lin (2001), Fluid and kinetics signatures of reconnection at the dawn tail magnetopause: Wind observations, *J. Geophys. Res.*, *106*, 25,489.

Phan, T. D., et al. (2006), A magnetic reconnection X-line extending more than 390 Earth radii in the solar wind, *Nature*, *439*, 175, doi:10.1038/nature04393.

Pritchett, P. L. (2001), Collisionless magnetic reconnection in a three-dimensional open system, *J. Geophys. Res.*, *106*, 25,961.

Sonnerup, B. U. O. (1979), Magnetic reconnection, in *Solar System Plasma Physics*, vol. 3, edited by E. N. Parker, C. F. Kennel, and L. J. Lanzrotti, p. 45, Elsevier, New York.

Sonnerup, B. U. O., G. Paschmann, I. Papamastorakis, N. Sckopke, G. Haerendel, S. J. Bame, J. R. Asbridge, J. T. Gosling, and C. T. Russell (1981), Evidence for magnetic field reconnection at the Earth's magnetopause, *J. Geophys. Res.*, *86*, 10,049.

Sonnerup, B. U. O., I. Papamastorakis, G. Paschmann, and H. Lühr (1990), The magnetopause for large magnetic shear: Analysis of convection electric fields from AMPTE/IRM, *J. Geophys. Res.*, *95*, 10,541.

Vaivads, A., Y. Khotyaintsev, M. André, A. Retinò, S. C. Buchert, B. N. Rogers, P. Décréau, G. Paschmann, and T. D. Phan (2004), Structure of the magnetic reconnection diffusion region from four spacecraft observations, *Phys. Rev. Lett.*, *93*(10), doi:10.1103/PhysRevLett.93.105001.

Wygant, J. R., et al. (2005), Cluster observations of an intense normal component of the electric field at a thin reconnecting current sheet in the tail and its role in the shock-like acceleration of the ion fluid into the separatrix region, *J. Geophys. Res.*, *110*, A09206, doi:10.1029/2004JA010708.

F. S. Mozer, Space Sciences Laboratory, Department of Physics, University of California, 366 LeConte Hall #7300, Berkeley, CA 94720, USA. (fmozer@ssl.berkeley.edu)

A. Retinò, Swedish Institute of Space Physics, Box 537, SE-75121